

Epitaxial Growth of ZnO Films on Ferroelectric YMnO₃ Films Deposited by The PLD Method

R. Arai, N. Shigemitsu, K. Masuko, T. Oshio, T. Yoshimura, A. Ashida, and N. Fujimura
 Graduate School of Engineering, Osaka Prefecture University, 1-1, Gakuen-cho, Sakai, Osaka 599-8531, JAPAN
 e-mail: fujim@ams.osakafu-u.ac.jp

The crystallinity and electrical properties of ZnO films grown on YMnO₃/Pt/sapphire substrate were investigated for realizing a piezoelectric/ferroelectric gate transistor. The x-ray diffraction (XRD) profiles of ϕ scan revealed that the ZnO layer was epitaxially grown on YMnO₃ with 30° rotation. The epitaxial relationships were (0001)ZnO // (0001)YMnO₃ and [10-10]ZnO // [10-10]YMnO₃. The carrier concentration and the hall mobility of the ZnO layer on YMnO₃/YSZ were $2.5 \times 10^{17} \text{ cm}^{-3}$ and $65 \text{ cm}^2/\text{Vs}$, respectively. The Au/Ti/ZnO/YMnO₃/Pt/sapphire capacitor exhibits ferroelectric-type hysteresis in the capacitance-voltage characteristics with a memory window of 0.8 V.

Key words: ZnO, YMnO₃, ferroelectric, piezoelectric, FET

1. INTRODUCTION

Ferroelectric thin films have been extensively studied for non-volatile memory device applications. Metal/ferroelectric/semiconductor field-effect transistors (MFS-FETs) have attracted much attention for further integration of memory. MFS memories, in which the gate voltage is controlled by the spontaneous polarization of ferroelectric material in addition to the external bias voltage, have potential advantages such as high switching speed, non-volatility and non-destructive read-out. However, they have a serious problem, which is the formation of an amorphous SiO₂ layer with a low dielectric constant at the interface between ferroelectric oxide and Si [1]. Therefore, it is very important to obtain a sharp interface without any dielectric layers, with low dielectric constant at the interface between ferroelectric oxide and the semiconductor.

The use of an oxide semiconductor is one of the solutions for the problem. Furthermore, it is expected that the spontaneous polarization and piezoelectricity of an oxide semiconductor enhances a strong carrier confinement at the ferroelectric/piezoelectric-semiconductor interface.

In this study, ZnO was chosen as a channel layer since it has the largest spontaneous polarization and piezoelectricity among the various semiconductors. YMnO₃ was selected as a ferroelectric gate material, since it has a hexagonal structure as does ZnO and the in-plane lattice mismatch is almost 5.2%. We have previously reported on the epitaxial YMnO₃ films on Pt/sapphire substrate with excellent ferroelectricity [2]. As a fundamental investigation of a bottom-gate type ZnO/YMnO₃-FET operating in the enhancement mode, we calculated the simulation of drain current-drain voltage characteristics [3]. In this paper, preparation of ZnO/YMnO₃/Pt/sapphire substrate is carried out and the structural and electrical properties of the capacitor are described.

2. EXPERIMENTAL DETAILS

To obtain a clean and highly crystallized surface with a step and terrace structure, the c-cut sapphire was annealed in air at 1050°C for 5 hours. Pt as a bottom electrode was deposited at 600°C by rf magnetron sputtering. A YMnO₃

layer was prepared by the pulsed laser deposition (PLD) method with ArF excimer laser ($\lambda=193\text{nm}$). Growth temperature and the O₂ partial pressure during deposition were 740°C and 5×10^{-3} Torr, respectively. Although ZnO films were also deposited by the PLD method, a KrF excimer laser (248 nm) was used. A 100-nm-thick ZnO was grown on the epitaxial YMnO₃/Pt/sapphire at the substrate temperature (T_s) ranging from 500°C to 650°C in a fixed gas pressure of 1×10^{-4} Torr.

Crystallinity of ZnO and YMnO₃ and the epitaxial relationship of orientations between each layer were evaluated by x-ray diffraction (XRD). The resistivity, carrier concentration, and electron mobility of the ZnO layers were evaluated by hall measurement. The surface morphology of the films was observed by an atomic force microscope (AFM). The polarization-electric field (P-E) characteristics of the Pt/YMnO₃/Pt/sapphire capacitor were measured using a Sawyer-Tower circuit. The capacitance-voltage characteristics were measured using an LCR meter (HP 4284A) with small ac amplitude of 25 mV from 20 Hz to 1 MHz.

3. RESULTS AND DISCUSSION

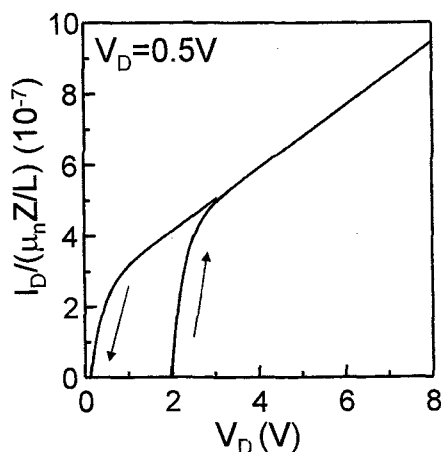


Fig. 1. The simulated drain current-drain voltage (I_D - V_{DS}) characteristics for the bottom-gate type ZnO-TFTs using ferroelectric YMnO₃.

At the beginning of the study, device performance was calculated to optimize the device structure. Fig. 1 shows the simulated drain current-drain voltage (I_D - V_{DS}) characteristics for the bottom-gate type ZnO-TFTs using ferroelectric dielectric YMnO₃. The width-to-length ratio of the gate is 5:1. The surface charge density of the ferroelectric YMnO₃ film was calculated by using Miller's formula. Miller's formula is described as follows:

$$Q_F = \epsilon_0 \epsilon_F V_F / d_F + P_s \tanh \left[\left(\frac{V_F \pm E_C}{d_F} \right) \ln \left\{ \frac{1 + P_r / P}{1 - P_r / P} \right\} / \pm E_C \right]$$

where ϵ_0 , ϵ_F , P_s , P_r and d_F are the permittivity, dielectric constant, saturated polarization, remnant polarization, and thickness of the ferroelectric layer, respectively. The direction of the spontaneous polarization of ZnO depends on the surface polarity of YMnO₃. Since ZnO grows on YMnO₃ under the O-terminated condition, in this calculation, the direction of the spontaneous polarizations of ZnO and the YMnO₃ was supposed to be toward the up direction along the c-axis. Used spontaneous polarizations of ZnO and YMnO₃ were -0.057 C/m^2 [4] and -0.043 C/m^2 , respectively. This TFT operates as an enhancement mode due to the direction of the spontaneous polarization of ZnO. Based on the simulated I_D - V_{DS} characteristic, we decided to fabricate the bottom-gate type TFT.

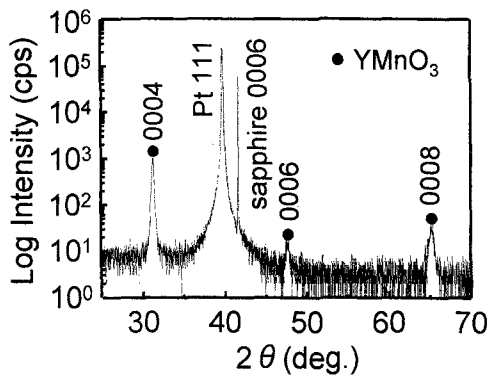


Fig. 2. XRD pattern of 100-nm-thick YMnO₃ thin film on epitaxial Pt/sapphire substrate.

A YMnO₃ layer was prepared with an ArF excimer laser. Growth temperature and the O₂ partial pressure during deposition were 740°C and 5×10^{-3} Torr, respectively. Detailed deposition conditions were reported elsewhere [2]. Figure 2 shows the XRD pattern of 100-nm-thick YMnO₃ thin film on epitaxial Pt/sapphire substrate. Diffraction

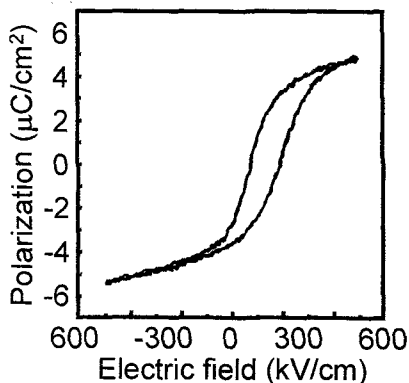


Fig. 3. P-E characteristic of the YMnO₃ grown on epitaxial Pt/sapphire.

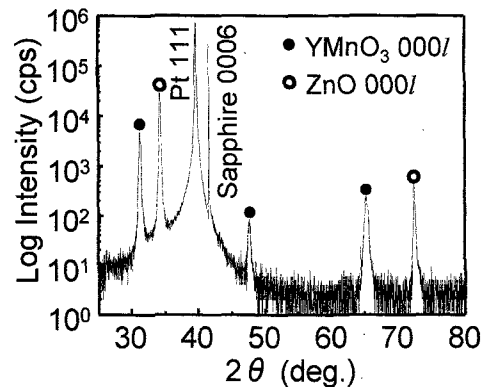


Fig. 4. XRD pattern of ZnO/YMnO₃/Pt/sapphire stacked layers.

peaks corresponding to 000/ YMnO₃ can be recognized, indicating that the film has a highly preferred orientation. We also measured XRD ϕ scan to confirm the epitaxial relationships. The epitaxial relationships are revealed as (0001)YMnO₃//(111)Pt//(0001)sapphire and [10-10]YMnO₃//[110]Pt//[10-10]sapphire. Since the YMnO₃ epitaxial film with excellent crystallinity was obtained on epitaxial Pt/sapphire substrates, the dielectric properties were measured. The P-E characteristics of the YMnO₃ are shown in Figure 3. Although the hysteresis loop is a little imprinted, the remnant polarization of $3.9 \mu\text{C/cm}^2$ and the saturated polarization of $4.2 \mu\text{C/cm}^2$ are almost identical to the reported spontaneous polarization of single crystal ($5.5 \mu\text{C/cm}^2$) [5]. The AFM image of the YMnO₃ film showed a smooth surface with the root-mean square roughness of 0.31 nm.

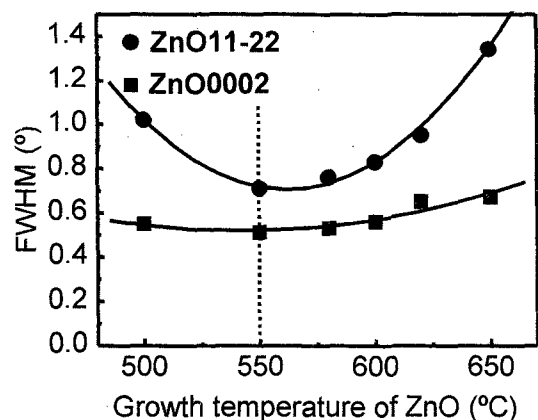


Fig. 5. FWHM of the rocking curves of the 0002(■) and 11-22(●) diffractions as a function of deposition temperature.

On the top of the epitaxial YMnO₃/Pt/sapphire substrate, ZnO films were deposited by PLD method with a KrF excimer laser. The substrate temperature was changed from 500 °C to 650 °C in the fixed gas pressure of 1×10^{-4} Torr. Fig. 4 shows the XRD pattern of ZnO/YMnO₃/Pt/sapphire stacked structure. The deposition temperature of the ZnO film was 550 °C. Diffraction peaks corresponding to the 000/ diffractions from YMnO₃ and ZnO were observed. No diffractions from other orientation or other phases were recognized. The ZnO layer has excellent crystallinity with the full width at half maximum value

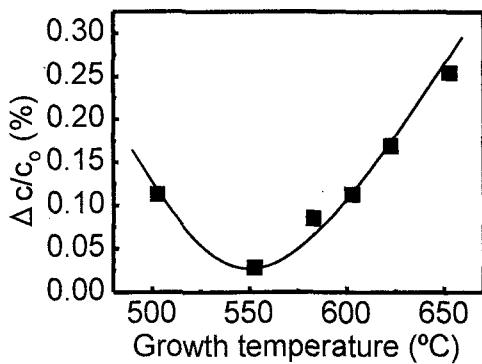


Fig. 6. Change in the relative lattice constant along the c-axis of ZnO as a function of deposition temperature.

(FWHM) of 0002 rocking curve of about 0.6°.

Figure 5 shows the change in FWHM of the rocking curve using 0002 and 11-22 diffractions as a function of deposition temperature of ZnO films grown on YMnO₃/Pt/sapphire substrate. The FWHM of the 0002 rocking curve slightly changes in the range from 0.55° to 0.61°. On the other hand, the FWHM of the 11-22 rocking curve changes depending on the deposition temperature, which indicates that the temperature is more effective for the in-plane orientation compared to the out-of-plane orientation.

Figure 6 shows change in the relative lattice constant along the c-axis ($\Delta c/c_0$) of ZnO normalized by the length of bulk value ($c_0=5.204 \text{ \AA}$) as a function of deposition temperature. As can be seen, $\Delta c/c_0$ of the film deposited at $T_S = 550^\circ\text{C}$ reaches to zero indicating that the lattice of the film is almost relaxed and the c-parameter is closest to that of bulk value.

Figure 7 shows ϕ scan of XRD of ZnO layer deposited at 550 °C on YMnO₃/Pt/sapphire. Six folds symmetry is observed. It is also recognized that ZnO grows on YMnO₃ with 30° rotation. The epitaxial relationships are (0001)ZnO// (0001)YMnO₃ and [10-10]ZnO//[10-10]YMnO₃. Figure 8 shows the atomic arrangement of (0001)ZnO

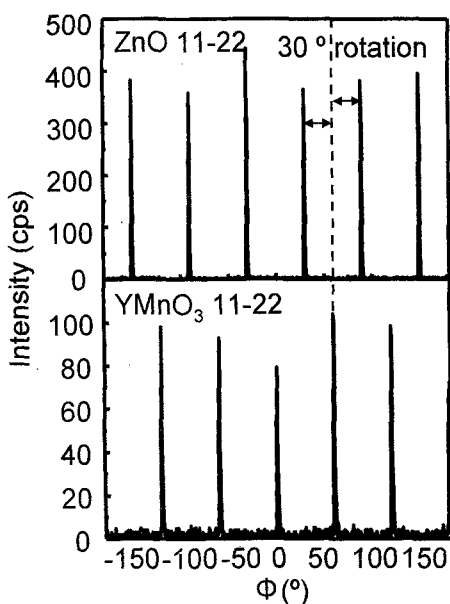


Fig. 7. ϕ scan of XRD of ZnO layer deposited at 550 °C on YMnO₃/Pt/sapphire.

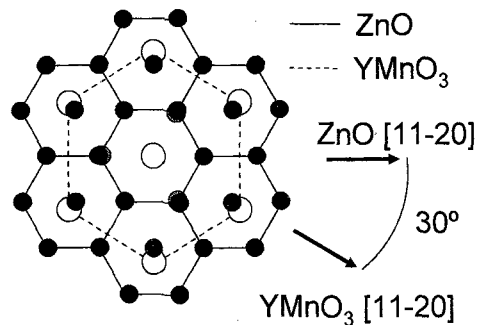


Fig. 8. Atomic arrangement of (0001)ZnO superimposed on that of (0001)YMnO₃.

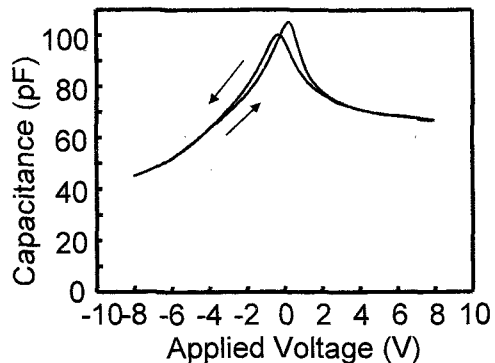


Fig. 9. Typical C-V characteristics of Au/Ti/ZnO/YMnO₃/Pt/sapphire structure measured at 1MHz.

superimposed on that of (0001)YMnO₃. In this configuration, the lattice mismatch can be reduced from 15% to 5.2%. Therefore, the interfacial energy minimization is responsible for the 30° rotated in-plane epitaxial orientation relationships.

To evaluate the carrier transport property of ZnO grown on YMnO₃ without bottom-electrode, ZnO was deposited on YMnO₃/yttria-stabilized zirconia (YSZ). (111)YSZ substrates were annealed at 1350°C for 3 hours in air in order to obtain an atomically flat surface with step and terrace structure [6]. The deposition conditions of ZnO and YMnO₃ films are identical to those for the Pt/sapphire substrate. ZnO film on YMnO₃/YSZ showed hall mobility of 65 cm²/V s and carrier concentration of $2.5 \times 10^{17} \text{ cm}^{-3}$. In fact, it was necessary to reduce the carrier concentration of ZnO films for the TFT operation.

Typical C-V characteristics of Au/Ti/ZnO/YMnO₃/Pt/sapphire structure measured at 1 MHz are shown in fig. 9. The applied bias voltage was swept at the fixed rate of 0.1 Vs⁻¹ from -8 to +8 V and +8 to -8 V. Counterclockwise ferroelectric hysteresis loops were observed. The obtained memory window of 0.8 V is identical to that expected from the coercive voltage of YMnO₃ in metal/ferroelectric/metal structure. Based on these results, we are sure that the ferroelectric hysteresis of YMnO₃ controls the surface potential of the ZnO layer.

4. CONCLUSIONS

Epitaxially-grown ZnO/YMnO₃ films on Pt/sapphire and YSZ were obtained. The epitaxial relationships are (0001) ZnO// (0001) YMnO₃ and [10-10] ZnO// [10-10] YMnO₃.

This 30° rotated in-plane epitaxial relationship is caused by reducing the lattice mismatch. T_s of ZnO is more effective for in-plane orientation distribution and the deposition at 550 °C is the optimal T_s of ZnO so as to reduce the lattice expansion and orientation distribution. The hall mobility and the carrier concentration of ZnO films on YMnO₃/YSZ were 65 cm²/V s and 2.5 × 10¹⁷ cm⁻³, respectively. In fact, it was necessary to reduce the carrier concentration of ZnO films for the TFT operation.

The Au/Ti/ZnO/YMnO₃/Pt/sapphire capacitor with back-gate structure exhibits an anticlockwise C-V hysteresis with the memory window of 0.8 V. It is expected that the ferroelectric hysteresis of YMnO₃ controls the surface potential of the ZnO layer.

5. REFERENCES

- [1] Y. Shinichi, S. Tanimoto, T. Goto, K. Kurosawa and Y. Tarui, *Jpn. J. Appl. Phys.*, **33** 5172 (1994).
- [2] N. Shigemitsu, H. Sakata, D. Ito, T. Yoshimura, A. Ashida, and N. Fujimura, *Jpn. J. Appl. Phys.*, **43** 6613 (2004).
- [3] Y. F. Chen, S. K. Hong, H. J. Ko, V. Kirshner, H. Wenisch, T. Yao. K. Inaba, and Y. Segawa, *Appl. Phys. Lett.*, **78** 3352 (2001).
- [4] B. Fabio, F. Vincenzo, and V. David, *Phys. Rev. B*, **56** 10024 (1997).
- [5] V. Peskov, A. Borovik-Romanov, T. Sokolova, and E. Silin, *Nucl. Instrum. Methods A*, **353**, 184 (1994).
- [6] H. Ohta, M. Orita, M. Hirano, H. Tanji, H. Kawazoe, and H. Hosono, *Appl. Phys. Lett.*, **76** 2740 (2000).

(Received January 11, 2005; Accepted February 2, 2005)